

RSC Advances



This is an *Accepted Manuscript*, which has been through the Royal Society of Chemistry peer review process and has been accepted for publication.

Accepted Manuscripts are published online shortly after acceptance, before technical editing, formatting and proof reading. Using this free service, authors can make their results available to the community, in citable form, before we publish the edited article. This *Accepted Manuscript* will be replaced by the edited, formatted and paginated article as soon as this is available.

You can find more information about *Accepted Manuscripts* in the [Information for Authors](#).

Please note that technical editing may introduce minor changes to the text and/or graphics, which may alter content. The journal's standard [Terms & Conditions](#) and the [Ethical guidelines](#) still apply. In no event shall the Royal Society of Chemistry be held responsible for any errors or omissions in this *Accepted Manuscript* or any consequences arising from the use of any information it contains.

Functional Wound Dressing Materials with Highly Tunable Drug Release Properties

Tina MAVER^a, MPharm, Silvo HRIBERNIK^a, PhD, Tamilselvan MOHAN^{b,*}, PhD, prof.
Dragica Maja SMRKE^c, MD, PhD, assist. prof. Uroš MAVER^{d,⊕,*}, MPharm, PhD and prof.
Karin STANA-KLEINSCHEK^{a,*}, PhD

^a University of Maribor, Faculty of Mechanical Engineering, Laboratory for Characterisation and Processing of Polymers, Smetanova 17, SI-2000 Maribor, Slovenia

^b University of Graz, Institute for Chemistry, Heinrichstrasse 28, 8010 Graz, Austria

^c University Medical Centre Ljubljana, Zaloška cesta 2, SI-1000, Ljubljana, Slovenia

^d University of Maribor, Faculty of Medicine, Department of Pharmacology and Experimental Toxicology, Taborska ulica 8, SI-2000 Maribor, Slovenia

[⊕] Member of Institute of Palliative Medicine and Palliative Care, Faculty of Medicine, University of Maribor, 2000 Maribor, Slovenia

*Corresponding authors

Prof. Dr. Karin Stana-Kleinschek

University of Maribor, Faculty of Mechanical Engineering
Laboratory for Characterisation and Processing of Polymers
Smetanova 17, SI-2000 Maribor, Slovenia

karin.stana@um.si

Phone: +386 2 220 7881

Fax: +386 2 220 7990

Dr. Tamilselvan Mohan

University of Graz

Institute for Chemistry

Heinrichstrasse 28, 8010 Graz, Austria

tamilselvan.mohan@uni-graz.at

Phone: +43 316 380 5413

Assist. prof. dr. Uroš Maver

University of Maribor, Faculty of Medicine

Department of pharmacology and experimental toxicology

Taborska ulica 8, SI-2000 Maribor, Slovenia

uros.maver@um.si

Phone: +386 2 234 5823

Fax: +386 2 234 5923

Abstract

Wound dressings, capable of local controlled delivery of non-steroid anti-inflammatory pain-killing drugs (NSAIDs) to the wound bed, offer great potential to accelerate wound healing, hence increase the quality of patient life. With local NSAID delivery, unwanted side effects encountered in their systemic delivery, are drastically diminished. In this study, four functional fibrous wound dressing materials, namely viscose, alginate, sodium carboxymethyl cellulose (Na-CMC) and polyethylene terephthalate (PET) loaded with a NSAID, diclofenac sodium (DCF) are prepared, and their suitability to tune the release rate of DCF is evaluated. Through careful examination of material-drug combinations, in terms of their physicochemical properties (air permeability, wettability and water retention) and structural/morphological properties (infrared spectroscopy, wide angle X-ray scattering and scanning electron microscopy), possible wound care applications are proposed. *In vitro* release studies using an automated Franz diffusion cell system, combined with UV-Vis absorption spectroscopy for drug release profile determination, are performed as the final pre-formulation test. Results showed significant differences in the release profiles between different material-drug combinations, making the examined materials highly applicable for several wound care applications. The present study presents a novel cost effective approach for preparation of drug loaded wound dressing materials without a sacrifice in patient safety. Additionally, novel methods and material-drug combinations are introduced, paving the way for possible future wound treatment options.

Keywords: wound dressing, NSAID, diclofenac sodium, release tuning, *in vitro* drug release investigation

1 **1. Introduction**

2 A wound is commonly referred to as a skin injury caused by trauma or surgery. Wound
3 healing generally follows a well-defined yet complex cascade of processes commonly divided
4 into four main stages; coagulation, inflammation, cell proliferation with repair of the matrix,
5 and epithelialization with remodeling of the scarred tissue¹. Depending on the extent and
6 depth of skin damage, the entire healing process can last for several months². Among the most
7 important conditions affecting wound healing start, are the wound cleanliness, a suitable
8 blood supply, and the absence of necrotic leftovers and fibrin plaques³. Once the healing is
9 underway, an appropriate moisture balance and prevention of infections, as well as exudate
10 management, are necessary to assure effective healing⁴. Although multi-layered and multi-
11 functional wound dressings are not a novelty in wound care/healing process⁵, existing
12 products do not address the challenging issues in wound treatment, such as controlled
13 therapeutic action or wound type specific healing.

14 Different fiber forming polymers are often used as drug carriers, absorbents or as moisturizers
15 in wound dressings⁶. Their semi-crystalline structures, nano-, micro- and especially macro-
16 porosity allow them to incorporate, bind and release different amounts of active ingredients
17 according to their respective structural and physico-chemical properties⁷. The most commonly
18 used are PET, cellulose and its derivatives and regenerated cellulose such as viscose, as well
19 as other types of polysaccharides. PET is a hydrophobic polymer, which is often used as an
20 inert layer of the dressing, suitable for contact with the damaged skin⁸. Regenerated cellulose
21 (viscose) and cellulose derivatives (sodium salt of carboxymethyl cellulose, Na-CMC), as
22 well as alginate, are among the most common functional parts of different modern wound
23 dressings⁹. Their final formulation shapes range from fibers, non-woven materials and
24 hydrogels to foams⁸.

25 Lately, novel advanced wound dressing formulations are explored in order to achieve
26 controlled release and delivery of drugs to wound sites^{10, 11}. The release from such materials is
27 sparsely reported in literature with few clinical studies carried out to date^{12, 13}. Especially little
28 or almost no literature is available regarding the controlled wound type specific drug delivery
29 using polymeric drug loaded materials as dressings. Despite the well-known fact that different
30 wounds exhibit significantly altered wound bed conditions¹⁴, they provide different
31 physiological conditions for drug release. Polymer-based dressings employed for controlled
32 drug delivery to wounds include hydrogels such as poly(lactide-co-glycolide)¹⁵, poly(vinyl
33 pyrrolidone)¹⁶, poly(vinyl alcohol)¹⁷ and poly(hydroxylalkyl-methacrylates)¹⁸, polyurethane-
34 foam¹⁹, hydrocolloid²⁰ and alginate dressings²¹. Other polymeric dressings reported in
35 literature for this purpose include novel hybrid formulations prepared from hyaluronic acid²²,
36 collagen²³ and chitosan^{24,25}.

37 Drug release from polymeric formulations is mostly controlled by one or more physical
38 processes including (a) hydration of the polymer, (b) swelling and gel formation, (c) diffusion
39 of the drug through the matrix and (d) eventual erosion of the matrix²⁶. Since wounds exhibit
40 different extents of exudation, it is expected that wound specific healing can be achieved by
41 combining swelling, erosion and subsequent drug diffusion kinetics as part of the controlled
42 drug release mechanism. In fact, most of the recently researched materials intended for wound
43 dressings (either natural or synthetic) release incorporated drugs by a combined mechanism of
44 either two or three above mentioned principles^{27, 28}.

45 Non-steroid anti-inflammatory drugs (NSAIDs) are important drugs in relieving pain,
46 fighting fever and decreasing inflammation. However, both NSAIDs and their selective
47 cyclooxygenase-2 (COX-2) inhibitors inhibit PGE2 production, which might exacerbate
48 excessive scar formation, especially when used during the later proliferative phase.

49 Nevertheless, it was shown that pain reduction induced decrease in stress, can positively

50 affect wound healing, resulting in shortened healing times²⁹. Based on scientific and clinical
51 evidence, pain can significantly slow down the healing process (mostly through stress induced
52 release of hormones like cortisol and norepinephrine), which results in decreased patient
53 quality of life as well as in exponentially increased personal and public expenditures³⁰⁻³².
54 Mostly NSAIDs are taken through systemic administration (i.e., in the form of pills), whereas
55 several approaches have been and are researched towards their integration into different
56 wound dressing formulations³³⁻³⁶. Although antibiotics are not the preferred type of drugs for
57 local treatment due to possible resistance acquisition of commensal bacteria, there are several
58 interesting studies available about preparation of dressing, combining NSAIDs and
59 antimicrobials³⁷⁻³⁹.

60 The purpose of this study was therefore to prepare wound dressing materials with
61 incorporated NSAIDs and to study their efficiency related to material performance and drug
62 release. For this purpose, only commercially available and clinically approved materials were
63 used. Four wound dressing materials, widely differing in their ability to take up liquids,
64 namely sodium salt of carboxymethyl cellulose (Na-CMC), alginate (ALG), viscose and
65 polyethylene terephthalate (PET) were chosen and subsequently integrated or loaded with the
66 (NSAID), diclofenac (DCF). The structural and surface properties of the material-DCF
67 potential wound dressing combinations were analyzed in detail using contact angle, water
68 retention and air permeability measurements, wide angle X-ray diffraction (WAXS) and
69 scanning electron microscopy (SEM). The application potential of the chosen materials was
70 shown in the release of the NSAID DCF *in vitro* using Franz diffusion cell release studies
71 followed by quantification using UV-Vis absorption spectroscopy. Through preparation of
72 four different material-DCF combinations and their ability to release DCF, this study was
73 intended to assess the suitability of different wound dressing materials for effective and safe
74 pain reduction in relation to the treatment of different wound types. To our best knowledge,

75 WAXS was never before used in examination of novel wound dressing formulations. Our
76 study aimed at providing a novel approach towards preparation of cost effective drug loaded
77 wound dressing solutions without the sacrifice of patient safety. It also provides a possible
78 novel PET based wound dressing with potential for future wound care applications.

79

80 **2. Materials and methods**

81 **2.1. Materials**

82 Four commercially available materials differing in their surface properties (wettability and
83 composition) were used as wound dressings. Viscose nonwoven (specific surface area mass=
84 175 g/m^2) was purchased from KEMEX, Netherlands. Fibrous alginate (ALG) and
85 carboxymethyl cellulose (Na-CMC; commercial, clinically used, wound dressing Aquacel®)
86 nonwoven were purchased from Sigma-Aldrich, Slovenia and ConvaTec, USA, respectively.
87 Polyethylene terephthalate, PET (100%, specific surface area = 75 g/m^2) in the form of a
88 mesh (mesh size of 0.8 mm) was purchased from BETI, Slovenia. Diclofenac sodium (DCF)
89 was purchased from Sigma-Aldrich, Germany. All the materials were used as received
90 without any further modification prior to sample preparation or testing. Ultra-pure water (18.2
91 $\text{M}\Omega \text{ cm}$ at $25 \text{ }^\circ\text{C}$) from an ELGA PureLab water purification system (Veolia Water
92 Technologies, UK) was used for preparation of all solutions.

93 **2.2. Integration of drug molecules into wound dressing materials**

94 The wound dressing samples were cut into 1 x 1 cm squares and impregnated with DCF
95 (dissolved in ultra-pure water, 1 mg/ml) for 15 minutes. Afterwards, the samples were dried in
96 an oven at $50 \text{ }^\circ\text{C}$ for 5 minutes, cooled down to room temperature and finally flushed with
97 nitrogen gas. The as-prepared samples were immediately used for *in vitro* release testing and
98 characterization.

99 **2.3. Methods**

100 *2.3.1. The Powder water contact angle measurement*

101 The wettability of the wound dressing materials (with and without incorporated DCF) was
102 measured using the powder contact angle measurement method (CA), which was performed
103 on a Krüss K12 processor Tensiometer (Hamburg, Germany). For the measurements, the
104 samples were cut into 2 cm × 5 cm rectangular pieces and placed into a special sample holder.
105 Prior to measurement, the container with the liquid (n-heptane or water) was raised until the
106 sample edge touched the liquid surface. The samples' mass (m) changes as a function of time
107 (t) during the water adsorption phase were monitored. The initial slope of the function $m^2 = f$
108 (t) is known as the capillary velocity, which can be used for determination of the contact angle
109 between the solid (polymer sample) and water using a modified Washburn equation:

$$\cos \theta = \frac{m^2}{t} \cdot \frac{\eta}{\rho^2 \cdot \gamma \cdot c} \quad (1)$$

110 where θ is the contact angle between the solid and liquid phases, $\frac{m^2}{t}$ is the capillary velocity, η
111 is the liquid viscosity, ρ is the liquid density, γ is the surface tension of the liquid and c is a
112 material constant^{4, 5, 40}.

113 All measurements were performed on three independent samples at three different sample
114 regions. An average value was calculated and the standard error is reported.

115 *2.3.2. Water retention values*

116 The water retention value of the chosen materials was determined according to standard DIN
117 53 814. This method is based on determining the quantity of water that the sample can absorb
118 and retain under defined and strictly controlled conditions. The water retention value is
119 expressed as the ratio between the mass of water, retained in the sample after soaking (t = 2 h)
120 followed by centrifuging (20 minutes), and the mass of an absolutely dry sample (T = 105 °C,
121 t = 4 h). All measurements were performed in four parallels and an average value was
122 calculated.

123 *2.3.3. Moisture content*

124 The moisture content of the wound dressing materials was determined using a Halogen
125 Moisture Analyser HB43 (Mettler Toledo, Giessen, Germany). This was done using the
126 thermo-gravimetric principle: the samples' weight was measured before and after controlled
127 heating.

128 *2.3.4. Air permeability determination*

129 Air permeability determination of all materials was performed according to standard DIN 53
130 887 with the Karl Schröder apparatus (Karl Schröder KG, Germany). The pinned surface of
131 the sample was 20 cm², while the three-level air-flow measurer operated at 20 °C in 1013
132 mbar. During the measurement, the pressure at the surface of the sample and the temperature
133 were fixed at 1 mbar 23 °C, respectively.

134 The reference air permeability was calculated using the following equation (2):

$$V_N = f \cdot V_G \cdot \sqrt{\frac{P_U \cdot T_N}{P_N \cdot T_U}} \quad (2)$$

135 where V_N , P_N and T_N are the reference air permeability, pressure and temperature,
136 respectively, while V_G is the air permeability and P_U and T_U are the ambient pressure and
137 temperature and f is a factor for calculation, corresponding to a defined surface area.

138 *2.3.5. Determination of surface thickness*

139 The surface thicknesses of the samples was determined by the standard SIST ISO 5084, which
140 is defined as the perpendicular distance between the upper and lower side of the sample.

141 According to the measured thicknesses, the pore volumes and the heights of the air layers
142 were determined, which serve as the perfect basis for prediction of the samples voluminosity.
143 Measurements were performed using the Louis Schopper apparatus (Leipzig, Austria). The
144 thickness of the pressure plate and its surface area were 4 mm and 1000 mm² (with a diameter

145 of 35.68 mm), respectively. For each sample five measurements were performed and an
146 average value was calculated with an added standard error.

147 2.3.6. Attenuated total reflectance-infrared (ATR-IR) measurements

148 ATR-IR spectra were recorded using an Agilent Cary 630 FTIR spectrometer with the
149 diamond ATR module at a scan range of 4000-650 cm^{-1} . The scans were performed on three
150 different places in 8 repetitions on each sample surface before and after impregnation with
151 DCF and after the DCF release.

152 2.3.7. Wide angle X-ray scattering (WAXS) measurements

153 The WAXS experiments were performed using the S3-MICROpix solution of Hecus (Graz,
154 Austria) with a 50 Watt microsource Genix 2009 from Xenocs (Sassenage, France). The tube
155 consists of a copper anode with an emission wavelength of 1.5418 Å for the $K\alpha$ line. The
156 sample to detector distance was 291 mm with an angle of 4.2° . The optics are 3D for point
157 focus with a beam size of $50 \times 200 \mu\text{m}^2$ and a flux up to $4 \times 10^8 \text{ photons s}^{-1} \text{ mm}^{-2}$. The point
158 focus at the detector has a monochromatic WAXS resolution of $q(\text{min}) \geq 4 \cdot 10^{-3} \text{ \AA}^{-1}$. The
159 scattering vector (q) range is between 0.003 \AA^{-1} and 1.9 \AA^{-1} . As detection system, a 2D
160 Pilatus 100k Dectrics Detector (Baden, Switzerland) $34 \times 84 \text{ mm}^2$, with a pixel size of $172 \times$
161 $172 \mu\text{m}^2$ was used. A Nickel filter was used as semi-transparent primary beam stop. X'Pert
162 Highscore Plus (PANalytical B.V., Almelo, Netherlands) was used for analysis of the
163 obtained diffractograms.

164 2.3.8. Scanning electron microscopy (SEM)

165 The surface morphology of samples prior and after DCF impregnation was analyzed by SEM.
166 Prior to imaging, several single fibers were removed from all samples and pressed on a
167 double-sided adhesive carbon tape (SPI 116 Supplies, USA). Micrographs were taken using a
168 field emission scanning electron microscope (FE-SEM, Supra 35 VP, Carl Zeiss, Germany)
169 operated at 1 keV at room temperature.

170 2.3.9. *In vitro* release studies

171 *In vitro* drug release studies were performed using an Automated Transdermal Diffusion Cells
172 Sampling System (Logan System 912-6, Somerset, USA). The drug loaded samples were cut
173 into 1 x 1 cm squares and placed on the top of a cellulose acetate membrane. The receptor
174 compartment was filled with ultra-pure water and its temperature was maintained at 37 °C.
175 During the dissolution testing the medium was stirred continuously with a magnetic bar.
176 Samples were collected over a period of 24 h at different time intervals, while the
177 released/dissolved DCF concentration in the receptor medium was determined by UV-Vis
178 spectrophotometer (Cary 60 UV-Visible Spectrophotometer, Agilent, Germany) by
179 quantification of the absorption band at 276 nm.

180 The withdrawn sample volumes were replaced by fresh ultra-pure water. Due to sample
181 withdrawal, followed by sample dilution through media replacement, sink conditions were
182 assured. In calculation of concentrations using the Beer-Lambert Law, this dilution was
183 accounted for. All release studies were performed in three parallels. For the determination of
184 final incorporated DCF amount, pieces of the same size (1 x 1 cm squares) of each material
185 with incorporated drug were shredded and immersed into 20 ml absolute ethanol. After 48 h
186 of shaking, DCF concentration was determined by UV-Vis spectrophotometry. Furthermore,
187 to confirm the complete release of DCF the samples were dried in oven at 50 °C for 15
188 minutes and analyzed by ATR-IR.

189 To compare the differences in release rates of wound dressing materials loaded with DCF
190 drug, a regression analysis was performed using the GraphPad Prism Software Version 5.01.
191 A difference is considered to be significant, when the obtained p-value is lower than 0.05 ($p <$
192 0.05). The calculated p-values are given in the supporting information (Table S1).

193

194 3. Results and discussion

195 3.1. Wettability, water retention and moisture content of unloaded samples

196 Keeping the wound's surface moist is the fundamental principle of open wound treatment⁴¹.

197 Several methods can be applied to evaluate a material capability to assure appropriate

198 moisture in the wound bed. The common denominator of such measurements is

199 hydrophilicity, which is connected with the water contact angle and is reflected in the water

200 retention value, as well as in the materials moisture content. The water contact angles

201 (CA(H₂O)) and water retention values of unloaded wound dressing samples are shown in

202 **Figure 1.**

203 It is expected that CA(H₂O) are inversely proportional to the water retention values – the

204 larger the contact angle, the lower the water retention value, but while measuring the

205 mentioned on wound dressing materials, their 3D structure (often fibrous), in particular in the

206 case of PET and viscose materials, plays an important role in regulating their overall

207 hydrophilicity. The relation between CA(H₂O) and water retention values is therefore not

208 straightforward, as shown also in case of our results. The CA(H₂O) values demonstrate that

209 the most hydrophilic materials are clearly Na-CMC and alginate compared to other two

210 materials (viscose and PET). Alginate exhibits the lowest CA(H₂O): $54 \pm 3^\circ$, whereas the

211 measurement of the CA(H₂O) is not possible for Na-CMC (Aquacel®) due to its extremely

212 high soaking ability and hydrophilic nature, which is facilitated by a higher content of

213 carboxylic groups. The latter prevented us to determine the capillary velocity, and hence the

214 CA(H₂O) value for this sample. From literature it is clear that the contact angle of Na-CMC is

215 very dependent on the material type. A range of CA(H₂O) values from low to high can be

216 found in the literature^{42, 43}. Since we are not able to measure this value, probably due to Na-

217 CMC super-molecular structure that allows the material to form a gel-like structure, which

218 results in an extremely high water uptake, this value is missing in Figure 1. The PET sample,

219 as a known hydrophobic synthetic polymer, exhibited a CA(H₂O) of $90 \pm 4^\circ$ ⁴³. Viscose

220 (cellulose, regarded as a hydrophilic material) rather shows a higher CA(H₂O): $88 \pm 4^\circ$,
221 similar to PET. This increased CA(H₂O) can be attributed to complex structural properties of
222 cellulose fibers, such as two-phase regime composed of disordered accessible regions and
223 ordered crystalline regions, porous system with voids and interfibrillar interstices, fiber
224 orientation, etc.^{44, 45}

225 By far the highest water retention value was determined for the Na-CMC sample. Indeed, the
226 measured value is so high (1521%) that we have to present it in a separate diagram (Figure
227 2B) to allow for a clearer comparison of the other samples. The higher water retention values
228 of Na-CMC can be related to incorporation of a larger number of water molecules by its
229 ionisable carboxylic groups (-COO⁻). PET samples, on the other hand, exhibit the lowest
230 values for water retention due to their high hydrophobic character. The water is repelled from
231 its surface, and consequently, the resulting value can almost not be seen in Figure 1 (0.3%).

232 Alginate and viscose exhibit water retention values of 81% and 61%, respectively. These
233 values are in agreement with the values reported in literature for alginate⁴⁶ and viscose⁴. The
234 differences in their water retention properties can be attributed to their functional groups and
235 structural properties (porosity, degree of crystallinity and fiber orientation)^{45, 47}.

236 Moisture content measurement is an important feature, affecting our choice of drug host
237 materials in wound treatment, since it affects the final capacity to uptake fluids when applied
238 on the wound. On the other hand, the initial moisture content can seriously influence the
239 controlled release behavior due to porosity and changes in mechanical strength of the host
240 material. It also affects the release and distribution of drug molecules, especially considering
241 the drug molecules accessibility by the release media⁴⁸. More related discussion will be
242 presented in the section explaining drug release studies. The results of materials' moisture
243 content evaluation show a similar order among tested samples as for the CA(H₂O), except for
244 Na-CMC, for which CA(H₂O) could not be obtained. Na-CMC was initially in a dry form

245 than alginate, but exhibits in its pure form (out of the secondary packaging) a higher moisture
246 content than viscose and PET (**Table 1**). Based on the moisture content differences among the
247 used materials, extreme care is necessary during all other testing procedures in order to avoid
248 possible fluctuations in moisture during experimentation. Between measurements, all
249 materials were always placed into tightly sealed petri dishes and additionally sealed with
250 parafilm strips.

251 **3.2. Air permeability vs. thickness of samples**

252 A medical dressing must be permeable for gasses, but an excessive air permeability,
253 especially a higher moisture vapor transmission rate, could dry out the wound and have a
254 negative effect on healing. The latter is due to two mechanisms, either through direct impact
255 on newly formed cells (excessive drying of the wound bed causes cell death), or by resulting
256 in growing of the dressing into the wound⁴. The latter being a result of dressing interaction
257 with newly formed tissue, forming crusts and resulting in an unfavorable effect on the
258 wound's healing rate⁴⁹. Given the conditions of the testing method, air permeability is mostly
259 affected by the manufacturing method of the material (knitting and preparation of non-
260 woven), yet sample structure, chemical nature, as well as the samples' thickness must be
261 taken into account. Air permeability of the chosen materials was evaluated against the sample
262 flat thickness. The results are shown in **Figure 2**.

263 The expected correlation between thickness and air permeability, namely the thicker the
264 material, the lower is the air permeability, is obtained for Na-CMC and alginate. One could
265 argue that also viscose exhibits the same correlation, especially with the error bars counted in.
266 Based on these results, it is clear that the demonstrated air permeability of Na-CMC, alginate
267 and viscose are satisfactory for ensuring and maintaining optimal wound healing conditions.
268 On contrary, the results also clearly show an extremely high air permeability for PET, not
269 suitable for desired maintenance of a moist wound environment. PET is therefore only

270 applicable either in thicker layers or by preparation of multi-layered wound dressings
271 comprising additional materials.

272 **3.3. DCF incorporation and characterization: ATR-IR and WAXS spectroscopy of** 273 **samples**

274 ATR-IR spectroscopy is employed to access the chemical composition and structural
275 properties of the unloaded and DCF loaded wound dressing materials. A clear indication of
276 successful DCF incorporation in all samples (Na-CMC, alginate and viscose) except in the
277 case of PET can be seen from the IR spectra shown in **Figure 3**. For respective samples, these
278 are organized in a way allowing clear comparison of peaks that can be assigned to DCF. The
279 most important peaks are colored in green. A broad peak between 3700– 3000 cm^{-1} that
280 corresponds to OH vibration can be observed for all unloaded polysaccharide based materials
281 (Na-CMC, alginate and viscose). Pure PET, in contrast, can be characterized by –CH
282 vibrations at 2900 cm^{-1} and a typical finger print region (650-1700 cm^{-1})⁵⁰. After DCF doping
283 the emergence of several new peaks can be observed. Peaks that can be assigned to C-Cl
284 stretching vibrations are visible in the region of 650 – 780 cm^{-1} , while a band corresponding
285 to CH–N–CH bending vibration can be observed at 1376 cm^{-1} . At 1577 cm^{-1} , R=C=O
286 stretching vibration can be observed. Additional peaks corresponding to R-C=O stretching
287 and CH₂ bending are visible at 1305 and 1462 cm^{-1} . All these peaks are clearly visible for all
288 DCF loaded polysaccharide-based samples. This is an evidence that DCF is successfully
289 loaded into the used wound dressing materials regardless of the difference in their chemical
290 functionality and structural properties. Even though no peaks corresponding to DCF are
291 observed in the IR spectra for the PET sample, the presence of DCF is clearly evident from
292 the *in vitro* release results (see section 3.4) from this sample. A plausible reason can be that
293 the concentration of loaded DCF is too low to be detected by IR.

294 WAXS measurements, as an additional tool to support the findings of ATR-IR, is performed
295 to determine the structure of wound dressing materials as well as to detect the presence of
296 DCF in the samples (**Figure 4**). From the obtained diffractograms a DCF corresponding peak
297 around 21° , could be identified for all samples, although the latter is not that evident for the
298 PET sample with the lowest amount of incorporated DCF. This data fits well with ATR-IR
299 results (see Figure 3d), where almost no peaks related to DCF presence were noted. Apart
300 from the mentioned peak an additional peak around 26° could be observed for the viscose and
301 alginate DCF loaded samples, while the peak around 23° , also assigned to DCF, could be
302 observed for Na-CMC. Although WAXS is not a very frequently used method for this
303 purpose, it still has a higher potential for identification purposes as turned out also in our case.
304 Another useful information we could obtain from the measurements is an indication about
305 crystallinity of the sample. To confirm the overall sample crystallinity a more thorough
306 WAXS analysis would be necessary, but nevertheless, these results suggest that fractions of
307 all samples are amorphous and since the DCF assigned peak around 21° is evident even after
308 incorporation, the drug seems to remain in its crystal form. Most of the diffractograms exhibit
309 broad peaks, a characteristic contribution of the, structural components, lacking order. At this
310 point, we have to stress that the characterization was done at a limited range of angles,
311 therefore an explicit judgement is not possible. Since the crystal structure can significantly
312 affect the materials wetting properties⁵¹, WAXS results will be integrated also in the
313 explanation of the drug release later in the article.

314 **3.4. *In vitro* release studies**

315 In this study the targeted application is wound healing, where the drug release rates have to
316 efficiently follow the pharmacological specifics of different wound types. *In vitro* drug release
317 testing is therefore a very important evaluation method in order to evaluate the prepared
318 materials applicability in treatment of different wounds.

319 Results from the *in vitro* release testing, performed using an automated Franz diffusion cell
320 system, are depicted in **Figure 5**. Only the first 360 minutes of release are presented, since
321 this region exhibits the biggest differences between the used materials. The full release
322 profiles are given in the supporting information (Figure S1). The top figure (a) shows the
323 mass of the released drug (g/cm^2) for each DCF incorporated wound dressing material. The
324 reason for using such units lies in the suitability of such representation for possible clinical
325 application, where the dose can be easily calculated, based on the size of the dressing to be
326 applied. The bottom figure (b) exhibits the percentage of the released drug as a function of
327 time, which is important to immediately deduce the information about the release timeframe
328 of the incorporated dose. Since, acutely released higher doses could possibly lead to unwanted
329 side effects, such representation enables the planning of a safe and efficient treatment. In
330 general, both types of representation of the *in vitro* release results are highly useful, and
331 necessary to understand the release of the incorporated drug. Their combination renders
332 planning of treatments for specific wound types possible. The total amounts of the
333 incorporated DCF in the dressing after complete release (after 2880 minutes – 48h) are
334 presented in **Figure 6**. Significant differences in release profiles can be observed in both
335 representation types (Figure 5a and b). This is also reflected in p-value (significant difference,
336 see Table S1), which was calculated using a stepwise regression analysis. A p-value of 0.05 is
337 generally considered on the borderline of statistical significant difference. Thus, any p-value
338 that is below 0.05 is usually regarded as statistically significant. Obviously, in our case,
339 significant differences in release rates are observed for all wound dressing materials with
340 incorporated DCF (Table S1). Both alginate and Na-CMC samples, which are hydrophilic as
341 proven by $\text{CA}(\text{H}_2\text{O})$, showed a superior statistical significant differences ($p < 0.001$)
342 compared to those of hydrophobic PET and viscose samples, where a p-value below 0.05 is
343 obtained. The high p-values of viscose and PET samples indicates that their release profiles

344 are certainly different as compared to that of other two materials such as alginate and Na-
345 CMC, which can be clearly seen in Figure 5a. Despite following the same DCF incorporation
346 procedure, large differences were already observed in the amount of the incorporated drug per
347 surface area of the material (Figure 6). As mentioned above, these values are determined as
348 the released amount after the drug concentration did not change anymore.

349 Although the used drug in this study was not applied yet in a topical formulation clinically,
350 the desired dose can be calculated based on the presently commercially available and
351 clinically used DCF containing medicines for systemic use. The maximal dose in the latter is
352 75 mg per tablet. Since the bioavailability of the latter is in the range 30% locally, the desired
353 dose in the wound would be approximately 23 mg. Considering the *in vitro* release results, an
354 incorporation of DCF into a 10 x 10 cm squares alginate based dressing (alginate can
355 incorporate, and hence release the maximal DCF amount), would lead to a maximum possible
356 local concentration of around 20 mg. Considering the latter, we could claim that our
357 formulations could be efficient, as well as safe. But only further clinical studies can confirm
358 this assumption absolutely. As indicated in the introduction section, the literature only
359 sparsely reports the release from similar, whereas clinical studies are even more rare^{12, 13}.

360 There have been some reports about inclusion of ibuprofen, another NSAID into candidate
361 wound dressing materials^{34, 36, 52}, not to forget about Biatain® IBU, the commercial, clinically
362 used dressing with an incorporated NSAID^{19, 53}. The latter served as a starting consideration
363 point in our assumptions in regard of the dose.

364 While only a small drug amount (0.0282 mg/cm²) could be attached to PET, viscose (0.1289
365 mg/cm²), Na-CMC (0.2084 mg/cm²) and alginate (0.2426 mg/cm²) exhibited higher amounts
366 of incorporated DCF (Figure 6). Based on these results we are also able to judge the
367 efficiency of the initial impregnation process, where the samples are able to soak the
368 following percentages of DCF from solution, PET 2.8%, viscose 12.9%, Na-CMC 21%, and

369 alginate 24.3%. Na-CMC and alginate can for example host almost an eight-fold larger
370 amount of incorporated DCF compared to PET, which makes them more suitable for
371 applications on chronic wounds, where the dressing change frequency is lower. On contrary,
372 PET based dressings are probably not applicable in a single-layered form, since the
373 incorporated amount of the drug does not cover the desired drug dose. Instead, considering
374 figure 5b, PET could be very interesting for application on wounds with acute pain, where an
375 immediate effect is necessary. The release profile shows a release of 60% of the incorporated
376 drug in the first 5 minutes and reaches a plateau after 30 minutes. In the form of multi-layered
377 dressings with PET as the bottom layer (in touch with skin/wound) could significantly add to
378 the quality of patient treatment, since the pain would diminish immediately. Additionally, in
379 such multi-layered dressings a PET based first layer would be interesting for treatment of
380 wounds, where the dressing change frequency is high and is accompanied with pain, mainly
381 caused by the removal of freshly epithelized skin or due to over-sensitization of the
382 surrounding tissue as a consequence of inflammation⁵⁴.

383 Interestingly, the viscose dressing shows a release profile similar to PET. However in the case
384 of viscose 80% of the incorporated drug are released in the first 30 min, while the remaining
385 20% are released within 360 minutes. PET and viscose are very different chemically and
386 structurally, as well as exhibit different wettabilities. These leads to a huge difference in drug
387 uptake and importantly affects their possible usage in different applications. In addition, one
388 must account for a rather complex structure of the material as a whole. Namely, viscose fibers
389 are used in the form of a voluminous non-woven with plenty of space in-between individual
390 fibers, enabling significant drug incorporation. This is not the case with the thin PET mesh,
391 where only the actually exposed surface is capable to attach drug molecules. Its inert
392 structure, as well as nonporous form with a low surface area, allow for attachment or
393 incorporation of only small drug amounts (see Figure 6). Nevertheless, PET is still an

394 interesting material in wound care, since its inert surface prevents sticking to the wound. The
395 most suitable application of a PET dressing is therefore as the initial layer in contact with the
396 skin of multi-layered dressings. On the contrary, viscose in its non-woven form, allows on one
397 hand the incorporation of a larger amount of DCF (in the range of 450% more, when
398 compared to PET), and on the other, serves also a good absorbent for exudating wounds. The
399 exudate can often lead to infections, significantly slowing wound healing. Viscose has
400 therefore more options in regard of applicability. It can be used either as a lone dressing on
401 highly exudating painful wounds or as the second layer of multi-layered dressings, serving as
402 a drug reservoir in aid of the initial very fast release by the first PET layer.

403 Significantly higher doses of DCF could be incorporated into Na-CMC and alginate, also their
404 release profiles and p-values (see Table S1, supporting information) are quite different from
405 the other two materials (as discussed above), as well as differ also one from another. The
406 latter is especially evident in the drug release rate differences. Na-CMC releases
407 approximately 16% of DCF in 30 minutes, where the profile shows a turn and the release rate
408 decreases. After the first 30 minutes, DCF is released at a constant rate. Making a linear fit of
409 the curve from 30 minutes to the end, R^2 value of 0.96 is obtained (not shown). These results
410 suggest that incorporation of DCF into Na-CMC could assure a relatively constant DCF
411 supply for at least 24 h. Such prolonged release characteristics of Na-CMC together with the
412 highest capacity for binding and retaining water (see Figure 1), is highly desired in case of
413 chronic wound treatment, where pain is uninterruptedly present, the change of dressing is
414 infrequent and an extensive exudation is present. A high amount of exudate is already known
415 to limit the healing efficiency and therefore needs to be removed^{41,55}. Alginate on the other
416 hand shows a 45% DCF release in the first two hours of release. After 240 minutes a sudden
417 change in the release pattern is observed. In the next 60 minutes nearly 25% of DCF is
418 released. An explanation for this sudden burst release can be that Na^+ and Ca^{2+} in alginate

419 structure are exchanged, leading to the breakdown of the base material mesh⁵⁶. This material
420 degradation exposes an additional portion of the drug, which is then readily dissolved. The
421 last 20% of the drug are then released in 24 h. Such materials and release performance could
422 be interesting for wounds that are not moist enough on their own. Since alginate can hold a
423 significant amount of water (see Figure 1), the degradation of the material can lead to
424 moisturizing of the wound bed. Release from alginate could be described as a combination of
425 all the other observed profiles. Initial fast release during the first 2 h, followed by a diffusion
426 controlled release with another burst of DCF release from 240 to 300 minutes. Using such
427 host materials would be suitable for applications on wounds, where the pain caused by
428 dressing change could be alleviated with a bolus dose and maintained through the following
429 diffusion drug release, which would additionally reduce the injury induced pain sensation.

430 The results of the *in vitro* release are in accordance with other material properties, especially
431 with the materials wettability. Viscose and especially PET exhibit high contact angles. And
432 since DCF has a higher solubility in the used media, its fast release/dissolution in the media
433 comes not as a surprise. Contrary, alginate with an intermediate hydrophilicity and a contact
434 angle of 50°, which already incorporates a certain amount of water, releases the water soluble
435 DCF with a smaller release rate. Na-CMC with its very high water retention value and an
436 immeasurable contact angle, retains the drug even longer, since DCF has first to diffuse
437 through the material and then only to the media. Both, alginate and Na-CMC form also gels
438 (Na-CMC swells significantly), which also contributes to the smaller release rate than
439 compared to the other two materials. Finally, all materials seem appropriate candidates for
440 wound care, although for different wound types and PET only in combination with other
441 materials. A schematic representation of the material-drug combinations in relation to the
442 respective material *in vitro* release performance for wound care applications is shown in
443 Figure 7. To further verify the complete release of DCF, the samples collected after 24 h

444 release are analyzed by ATR-IR and WAXS (see the supporting material, Figure S2 and S3)
445 measurements.

446 The ATR-IR and WAXS spectra showed no characteristic peaks that can be assigned to DCF
447 in none of the used wound dressing materials collected after the *in vitro* release studies. The
448 latter is a clear indication that all the incorporated drug was released.

449 **3.5. SEM microscopy of sample surfaces prior and after *in vitro* release studies**

450 **Figure 8** shows the SEM morphology of all materials prior and after drug incorporation, as
451 well as after the *in vitro* release testing. SEM micrographs of pure drug particles are given in
452 the supporting document (Figure S5). All four chosen materials possess a fibrous form in their
453 unloaded state (Figure 8 – (U) left column). Some differences between materials are already
454 evident after DCF incorporation (Figure 8 – middle column). Na-CMC fibers seem to have
455 been partially broken apart into block like parts and the presence of drug particles cannot be
456 clearly observed. Another possibility is that this micrograph shows a broken part of the Na-
457 CMC polymer film that formed after drug incorporation. All other materials retained their
458 fibrous structure, while additional surface features can be observed that can be attributed to
459 the loading of DCF. On the PET-based samples, only a small amount of drug particles could
460 be observed on the surface, which is in agreement with the calculated (and measured) small
461 amount of the incorporated drug. On the contrary, alginate and viscose samples exhibit clearly
462 observable morphological changes on their respective surfaces. These corresponds well to the
463 measured larger amounts of incorporated DCF during *in vitro* dissolution testing. While it
464 seems that DCF is still in the form of crystals on the viscose fibers, a thin coating of DCF is
465 visible on alginate samples. This is also in agreement with the results of *in vitro* release
466 testing, where alginate clearly outperforms other materials in terms of the amount of the
467 incorporated drug and release performance. Additional drug particles on the surface are

468 smaller than crystals in the case of viscose (and PET), and as such, can improve the release
469 rate also by increasing the effective surface area.

470 Finally, SEM micrographs, taken after the *in vitro* drug release testing, are shown in Figure 8
471 – right. While the morphology of viscose and PET based samples retained their initial fibrillar
472 structure, there are significant differences evident for Na-CMC and alginate based samples.
473 Alginate fibers are probably partially deformed through degradation as a result of cation (Na^+
474 and Ca^{2+}) exchange in its structure. This did not lead to severe material disintegration, but to
475 an etching-like effect of the fiber surface as observed in Figure 8 - right. The most notable
476 changes after release are seen for Na-CMC, where the fibrous shape (and even the block-like
477 structure, present after DCF incorporation) disappeared completely. Through exposure of Na-
478 CMC to the dissolution media, Na-CMC swelled and formed a gel-like structure that
479 rigorously differs from the initial fibered structure. All mentioned observations seem to
480 correspond to the findings of other methods, especially with the results of *in vitro* drug release
481 testing.

482

483 **4. Conclusion**

484 Recent economic trends, as well as ongoing rationalizations in health care, dictate the
485 development of novel therapeutic approaches with lower overall costs without the sacrifice of
486 patient safety. This can be achieved through optimized treatment efficiency and lowered
487 hospitalization times. Wound care is no different from other health care sectors. We found
488 that a combination of optimal materials and potent drugs could lead to great improvement in
489 therapeutic efficiency of novel wound dressing materials, especially considering the different
490 treatment approaches for specific wounds. Our results not only show that significant
491 differences in the release profiles can be achieved by incorporating a NSAID, DCF into

- 492 different materials, but also indicate the importance of a careful drug host material
493 characterization in choosing the right material for the treatment of specific wounds.

Supporting Information

Supporting Information is available from the Royal Society of Chemistry or from the author.

Acknowledgements

The authors acknowledge the financial support from the Ministry of Higher Education, Science and Technology of the Republic of Slovenia, as well as the financial contributions from the WoodWisdom-NET+ funded project AEROWOOD with the grant number 3330-14-500041 and mnt-era.net funded project WoundSens with the grant number 3211-12-00002.

References

1. T. Velnar, T. Bailey and V. Smrkolj, *The Journal of international medical research*, 2009, **37**, 1528-1542.
2. E. A. Gantwerker and D. B. Hom, *Facial plastic surgery clinics of North America*, 2011, **19**, 441-453.
3. L. G. Ovington, *Clin Dermatol*, 2007, **25**, 33-38.
4. T. Pivec, Z. Peršin, M. Kolar, T. Maver, A. Dobaj, A. Vesel, U. Maver and K. Stana-Kleinschek, *Text Res J*, 2013, **84**, 96-112.
5. Z. Peršin, U. Maver, T. Pivec, T. Maver, A. Vesel, M. Mozetič and K. Stana-Kleinschek, *Carbohydr Polym*, 2014, **100**, 55-64.
6. J. J. Elsner and M. Zilberman, *Acta Biomater*, 2009, **5**, 2872-2883.
7. K. Vowden and P. Vowden, *Surgery (Oxford)*, 2014, **32**, 462-467.
8. G. D. Mogoşanu and A. M. Grumezescu, *Int J Pharmaceut*, 2014, **463**, 127-136.
9. N. Mayet, Y. E. Choonara, P. Kumar, L. K. Tomar, C. Tyagi, L. C. Du Toit and V. Pillay, *J Pharm Sci*, 2014, **103**, 2211-2230.
10. M. Ignatova, I. Rashkov and N. Manolova, *Expert Opin Drug Deliv*, 2013, **10**, 469-483.
11. H. E. Thu, M. H. Zulfakar and S. F. Ng, *Int J Pharm*, 2012, **434**, 375-383.
12. S. Kordestani, M. Shahrezaee, M. N. Tahmasebi, H. Hajimahmodi, D. Haji Ghasemali and M. S. Abyaneh, *J Wound Care*, 2008, **17**, 323-327.
13. G. Casey, *Nurs Stand*, 2002, **17**, 49-53; quiz 54, 56.
14. J. S. Boateng, K. H. Matthews, H. N. E. Stevens and G. M. Eccleston, *J Pharm Sci*, 2008, **97**, 2892-2923.
15. D. S. Katti, K. W. Robinson, F. K. Ko and C. T. Laurencin, *Journal of Biomedical Materials Research Part B: Applied Biomaterials*, 2004, **70B**, 286-296.
16. A. S. Hoffman, *Advanced Drug Delivery Reviews*, 2002, **54**, 3-12.
17. M. Kietzmann and M. Braun, *Dtsch. Tierarztl. Wochenschr.*, 2006, **113**, 331-334.
18. M. D. Blanco, O. Garcia, C. Gomez, R. L. Sastre and J. M. Teijon, *J Pharm Pharmacol*, 2000, **52**, 1319-1325.
19. B. Jørgensen, G. J. Friis and F. Gottrup, *Wound Repair and Regeneration*, 2006, **14**, 233-239.
20. H. E. Thu, M. H. Zulfakar and S. F. Ng, *Int J Pharm*, 2012, **434**, 375-383.
21. F. Gu, B. Amsden and R. Neufeld, *J Control Release*, 2004, **96**, 463-472.
22. N. Shimizu, D. Ishida, A. Yamamoto, M. Kuroyanagi and Y. Kuroyanagi, *Journal of biomaterials science. Polymer edition*, 2014, **25**, 1278-1291.
23. T. Muthukumar, K. Anbarasu, D. Prakash and T. P. Sastry, *Colloids and surfaces. B, Biointerfaces*, 2014, **121**, 178-188.
24. P. Szweda, G. Gorczyca, R. Tylingo, J. Kurlenda, J. Kwiecinski and S. Milewski, *Journal of applied microbiology*, 2014, **117**, 634-642.

25. A. G. Richetta, C. Cantisani, V. W. Li, C. Mattozzi, L. Melis, F. De Gado, S. Giancristoforo, E. Silvestri and S. Calvieri, *Recent patents on inflammation & allergy drug discovery*, 2011, **5**, 150-154.
26. J. R. Weiser and W. M. Saltzman, *J Control Release*, 2014, **190**, 664-673.
27. S. Moritz, C. Wiegand, F. Wesarg, N. Hessler, F. A. Müller, D. Kralisch, U.-C. Hipler and D. Fischer, *Int J Pharmaceut*, 2014, **471**, 45-55.
28. A. M. Abdelgawad, S. M. Hudson and O. J. Rojas, *Carbohydr Polym*, 2014, **100**, 166-178.
29. P. Price, K. Fogh, C. Glynn, D. L. Krasner, J. Osterbrink and R. G. Sibbald, *Int Wound J*, 2007, **4 Suppl 1**, 1-3.
30. E. A. Gantwerker and D. B. Hom, *Clin Plast Surg*, 2012, **39**, 85-97.
31. S. Petruyte, *Danish medical bulletin*, 2008, **55**, 72-77.
32. K. Solowiej, V. Mason and D. Upton, *J Wound Care*, 2010, **19**, 110-115.
33. T. Maver, U. Maver, F. Mostegel, T. Griesser, S. Spirk, D. Smrke and K. Stana-Kleinschek, *Cellulose*, 2015, **22**, 749-761.
34. K. Fogh, M. B. Andersen, M. Bischoff-Mikkelsen, R. Bause, M. Zutt, S. Schilling, J.-L. Schmutz, J. Borbujo, J. A. Jimenez, H. Cartier and B. Jørgensen, *Wound Repair and Regeneration*, 2012, **20**, 815-821.
35. B. Steffansen and S. P. K. Herping, *Int J Pharmaceut*, 2008, **364**, 150-155.
36. L. Vinklarkova, R. Masteikova, D. Vetchy, P. Dolezel and J. Bernatoniene, *BioMed research international*, 2015, **2015**, 892671.
37. J. S. Boateng, H. V. Pawar and J. Tetteh, *Int J Pharmaceut*, 2013, **441**, 181-191.
38. H. V. Pawar, J. Tetteh and J. S. Boateng, *Colloids and Surfaces B: Biointerfaces*, 2013, **102**, 102-110.
39. H. V. Pawar, J. S. Boateng, I. Ayensu and J. Tetteh, *J Pharm Sci*, 2014, **103**, 1720-1733.
40. H. J. Jacobasch, K. Grundke, E. Mäder, K. H. Freitag and U. Panzer, *J Adhes Sci Technol*, 1992, **6**, 1381-1396.
41. A. D. Widgerow, *Wound repair and regeneration : official publication of the Wound Healing Society [and] the European Tissue Repair Society*, 2011, **19**, 287-291.
42. C. Ramírez, I. Gallegos, M. Ihl and V. Bifani, *Journal of Food Engineering*, 2012, **109**, 424-429.
43. R. Kargl, T. Mohan, M. Bračić, M. Kulterer, A. Doliška, K. Stana-Kleinschek and V. Ribitsch, *Langmuir*, 2012, **28**, 11440-11447.
44. K. Stana-Kleinschek, V. Ribitsch, T. Kreze, M. Sfiligoj-Smole and Z. Persin, *Lenzinger Berichte*, 2003, **82**, 83-95.
45. W. E. Morton and J. W. S. Hearle, *Physical Properties of Textile Fibres: Fourth Edition*, 2008.
46. L. Fan, Y. Du, R. Huang, Q. Wang, X. Wang and L. Zhang, *J Appl Polym Sci*, 2005, **96**, 1625-1629.
47. D. W. Van Krevelen and K. Te Nijenhuis, *Properties of Polymers*, 2009.
48. I. Bravo-Osuna, C. Ferrero and M. R. Jiménez-Castellanos, *Eur J Pharm Biopharm*, 2008, **69**, 285-293.
49. F. K. Field and M. D. Kerstein, *Am J Surg*, 1994, **167**, 2S-6S.
50. A. Miyake, *Journal of Polymer Science*, 1959, **38**, 479-495.
51. C. F. Fan and T. Cagin, *J Chem Phys*, 1995, **103**, 9053-9061.
52. M. Romanelli, V. Dini, R. Polignano, P. Bonadeo and G. Maggio, *The Journal of dermatological treatment*, 2009, **20**, 19-26.
53. F. Gottrup, B. Jørgensen, T. Karlsmark, R. G. Sibbald, R. Rimdeika, K. Harding, P. Price, V. Venning, P. Vowden, M. Jünger, S. Wortmann, R. Sulcaite, G. Vilkevicius, T.-L. Ahokas, K. Ettler and M. Arenbergerova, *Int Wound J*, 2007, **4**, 24-34.

54. G. Wozniak, P. Mauckner, L. Steinstrasser and J. Dissemond, *Gefasschirurgie*, 2011, **16**, 281-290.
55. D. Ulrich, R. Smeets, F. Unglaub, M. Wöltje and N. Pallua, *Journal of Wound Ostomy & Continence Nursing*, 2011, **38**, 522-528
510.1097/WON.1090b1013e31822ad31290.
56. C. H. Goh, P. W. S. Heng and L. W. Chan, *Carbohydr Polym*, 2012, **87**, 1796-1802.

FIGURE CAPTIONS

Figure 1. A: The water contact angle and water retention properties of the wound dressing materials prior to drug incorporation. PET water retention value is not missing, but almost zero (0.3%), and therefore cannot be seen in the diagram. **B:** Na-CMC water retention value is shown in a separate diagram due to its much higher value, when compared to the other samples, shown in part A of the diagram. Water contact angle for Na-CMC (Aquacel®) could not be obtained.

Figure 2. Air permeability and thickness of the unloaded samples.

Figure 3. ATR – IR spectra of A) unloaded Na-CMC, DCF and Na-CMC with incorporated DCF, B) unloaded alginate, DCF and alginate with incorporated DCF, C) unloaded viscose, DCF, viscose with incorporated DCF and D) unloaded PET, DCF and PET with incorporated DCF.

Figure 4. WAXS diffractograms of samples prior and after DCF incorporation, as well as the reference diffractograms of DCF.

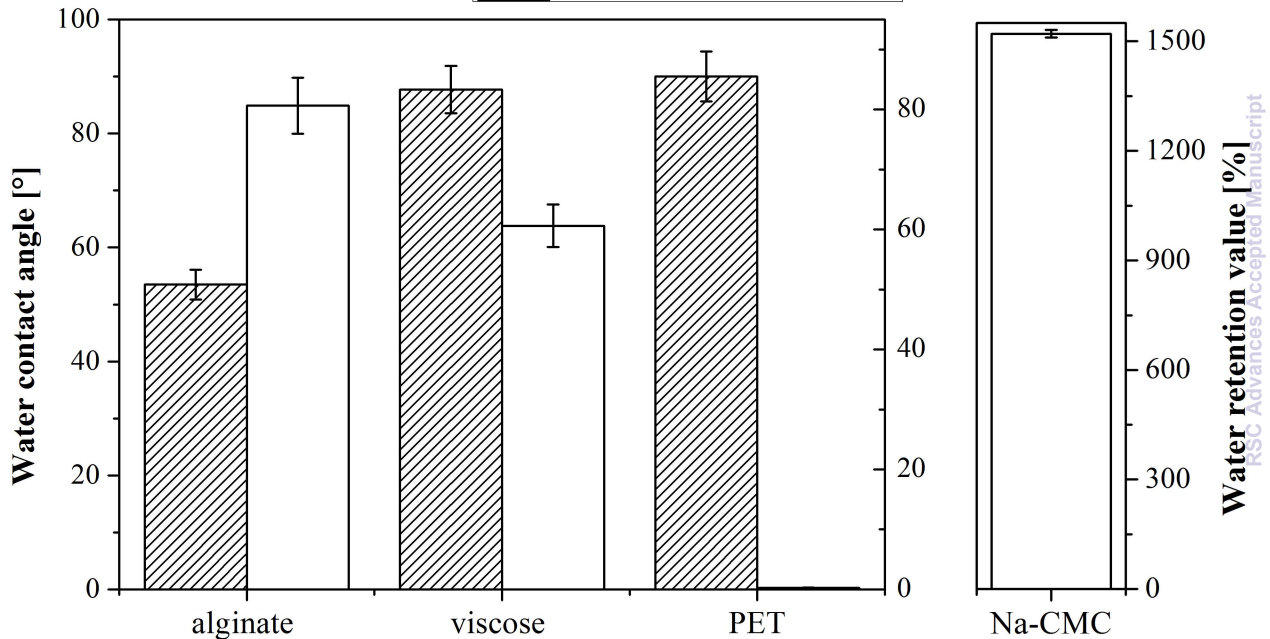
Figure 5. (a) amount of DCF released from a 1 x 1 cm squares model wound dressing and (b) percentage of released DCF, whereas the incorporated DCF amounts differ between the samples. Full release profiles are available as Figure S1 in the supporting information.

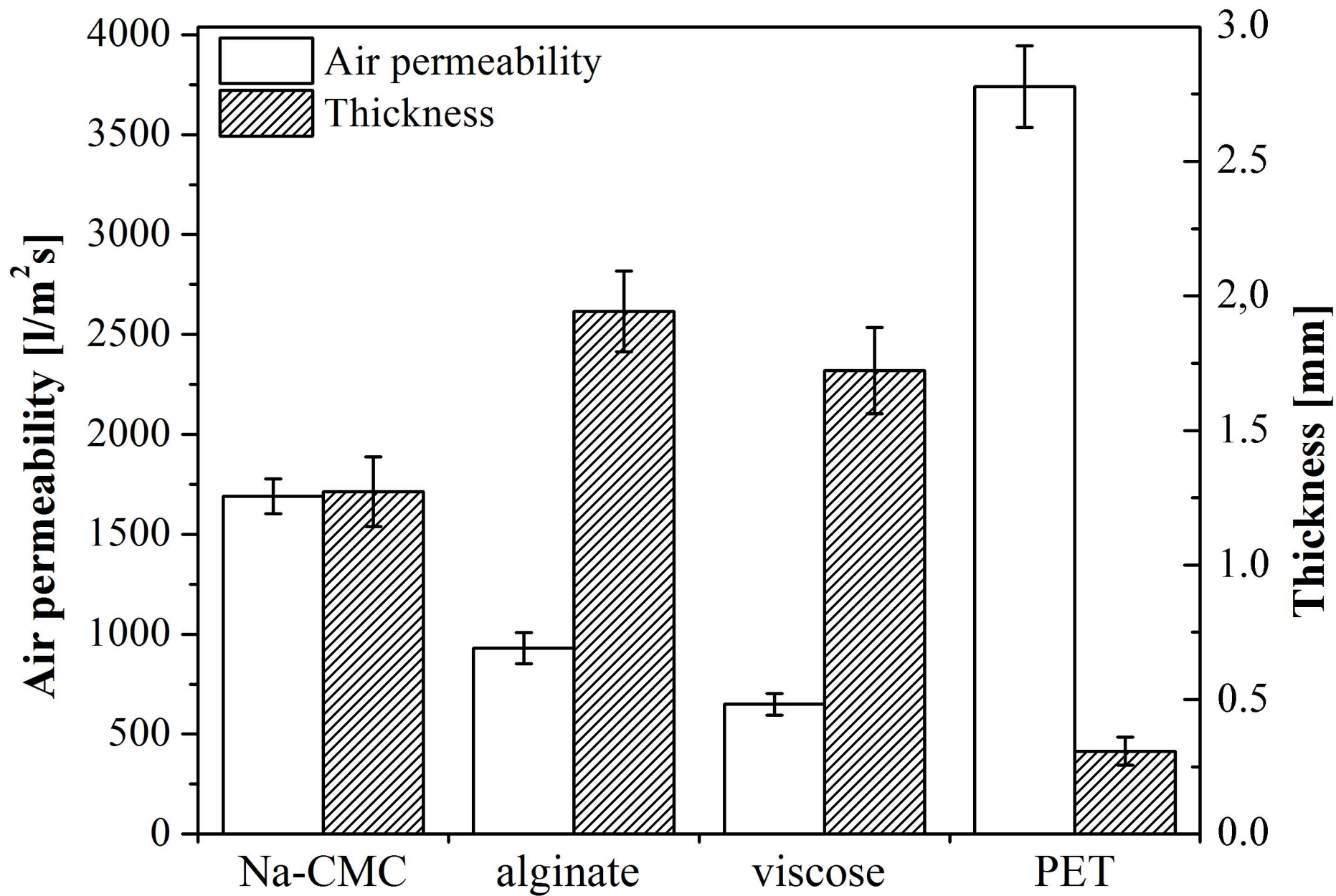
Figure 6. Total amounts of incorporated DCF in different wound dressing materials.

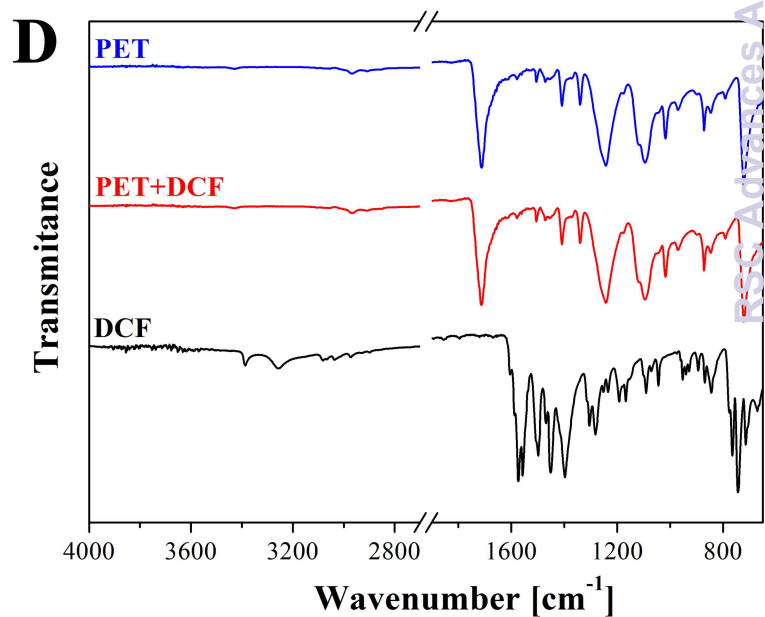
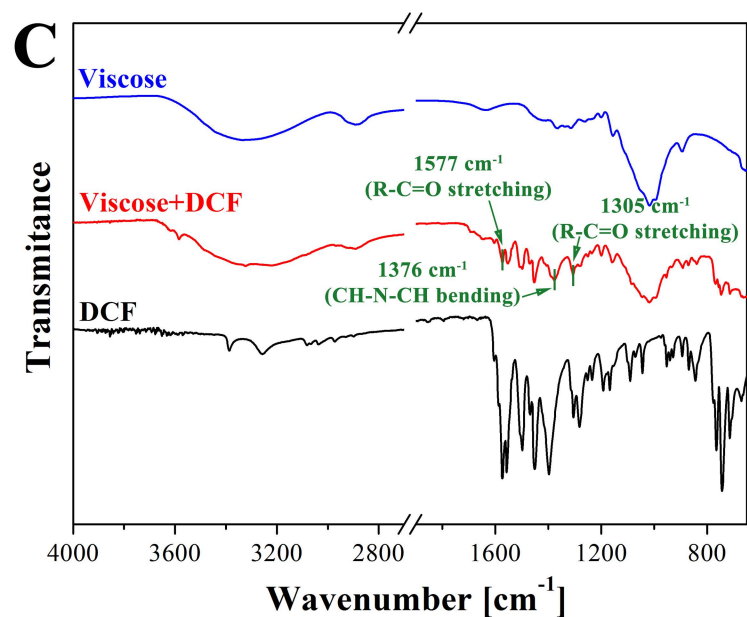
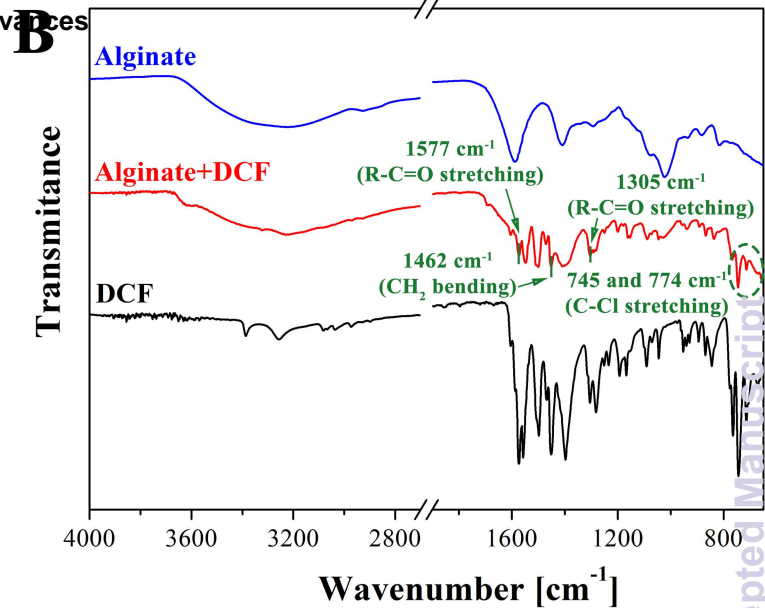
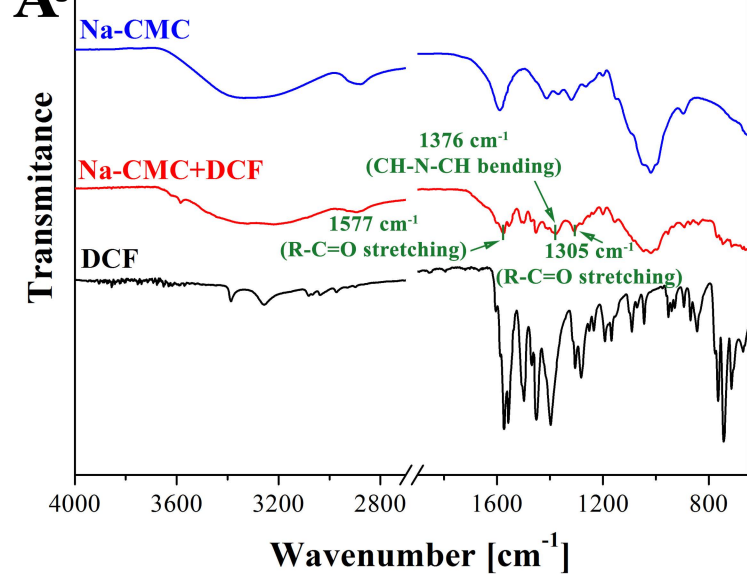
Figure 7. Schematic depiction of the material-drug combinations *in vitro* release performance and possible wound care applications. a) Na-CMC with incorporated DCF suitable in treatment of chronic wounds, b) Alginate with incorporated DCF for treatment of chronic wounds with

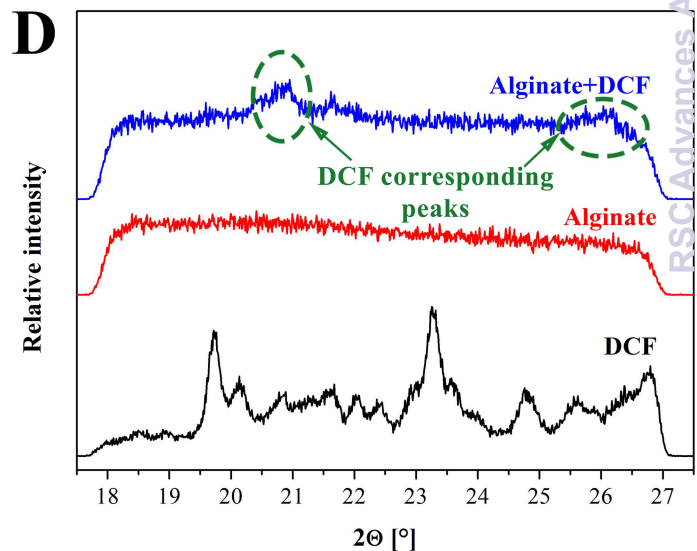
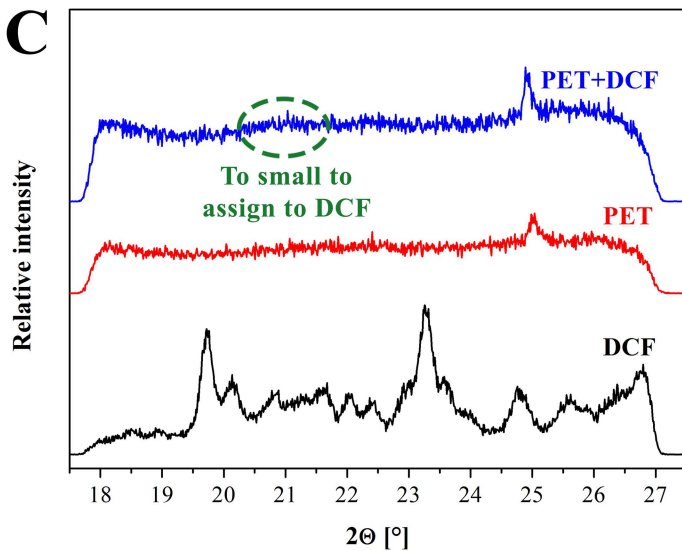
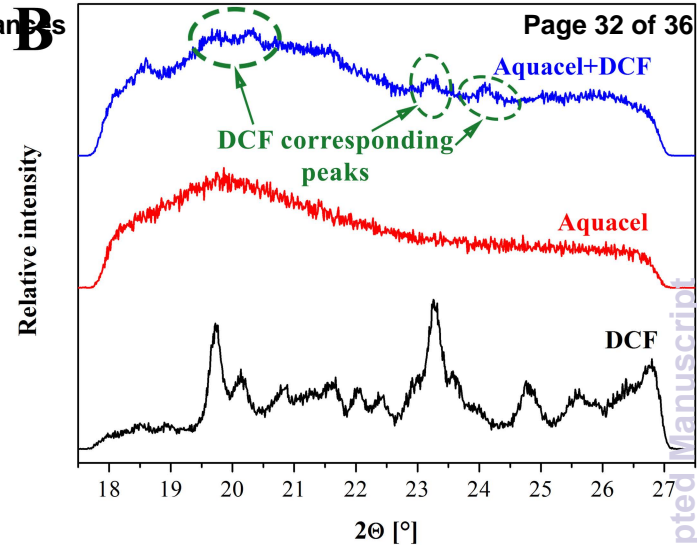
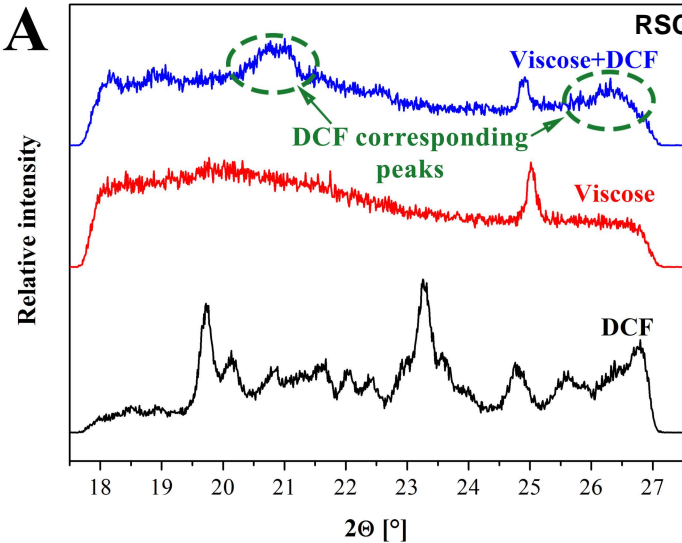
an even lower frequency of dressing change, c) Viscose with incorporated DCF for acute pain reduction and d) PET with incorporated DCF as an initial layer in contact with the skin for wounds, requiring frequent dressing change. The drug DCF is depicted in red, while the materials are shown in different colors and morphologies, according to their macroscopic nature. Shorter arrows exhibit a prolonged release, while longer arrows correspond to a faster release.

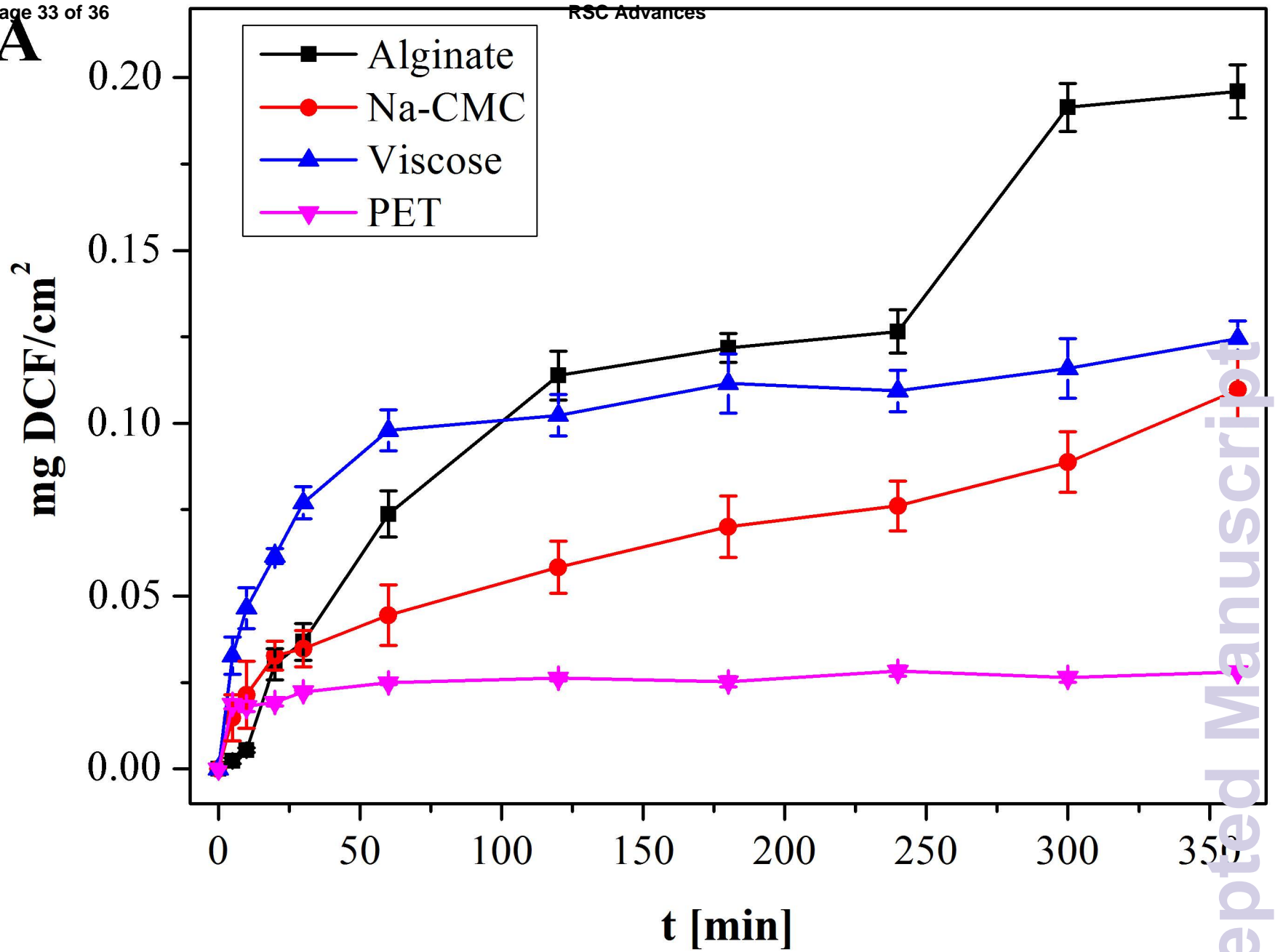
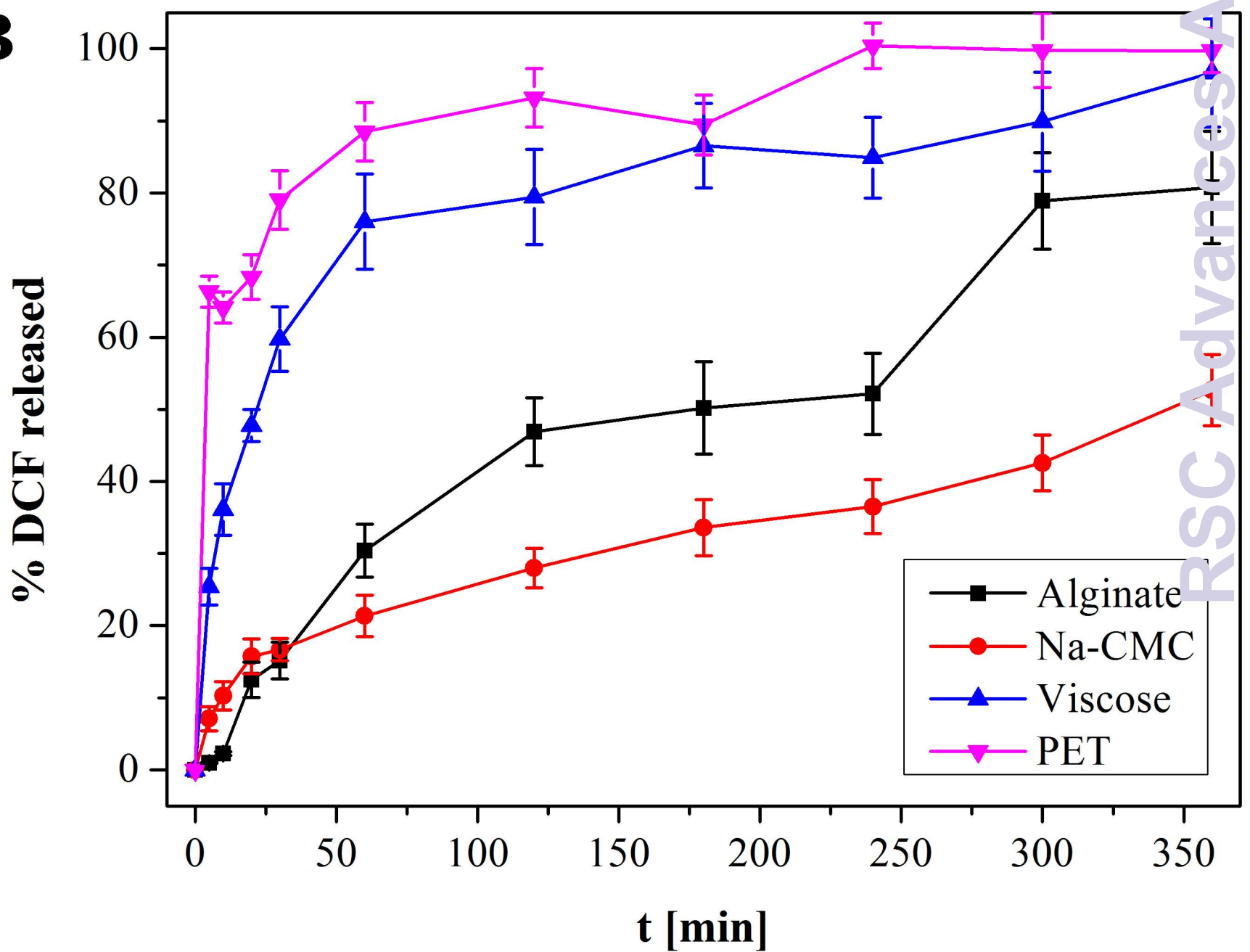
Figure 8. SEM micrographs of: LEFT - the unloaded (U) materials, MIDDLE - alginate, Na-CMC, viscose and PET impregnated with DCF (+DCF), RIGHT - alginate, Na-CMC, viscose and PET after the release studies (after). The used magnification was 10,000x.

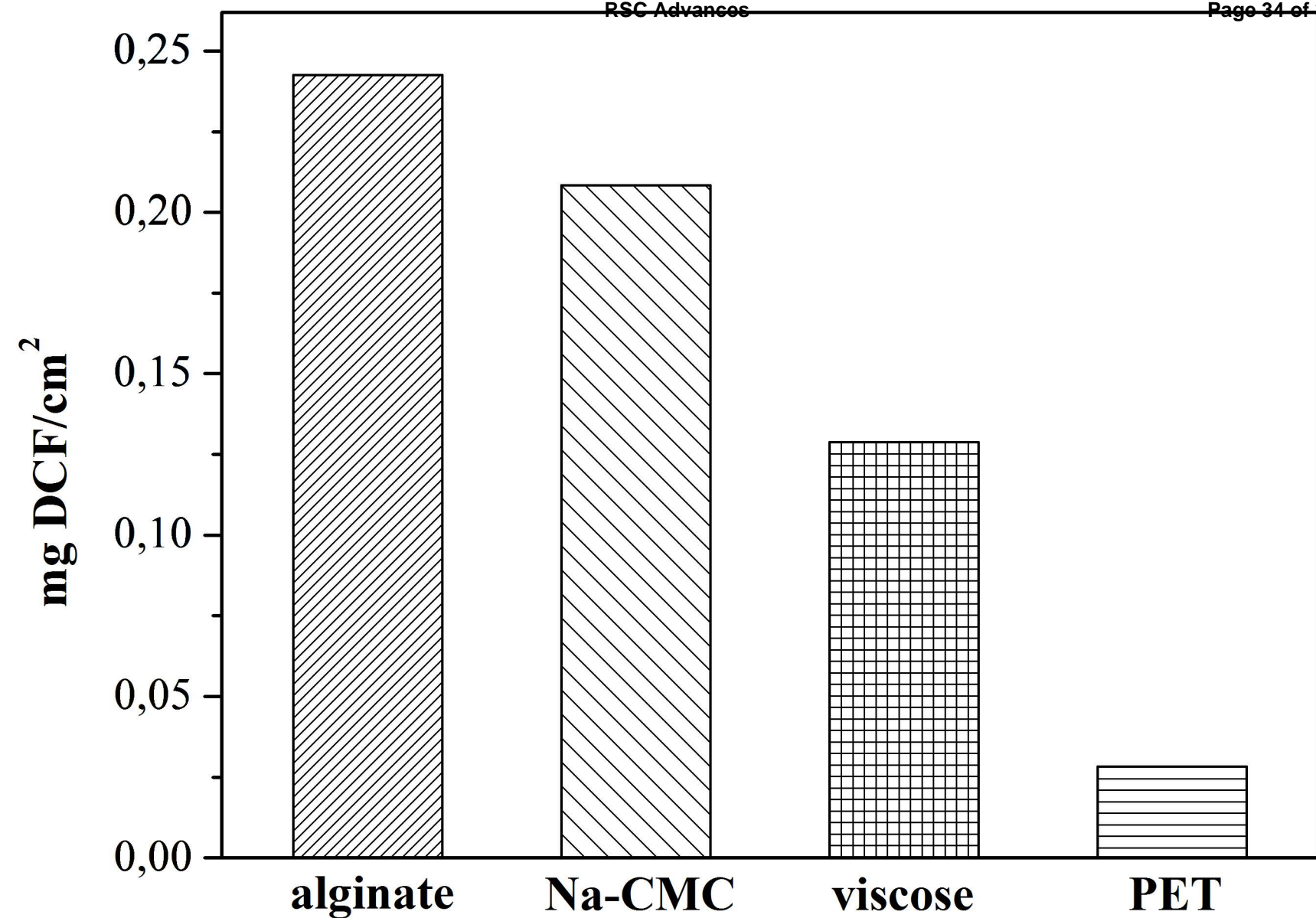


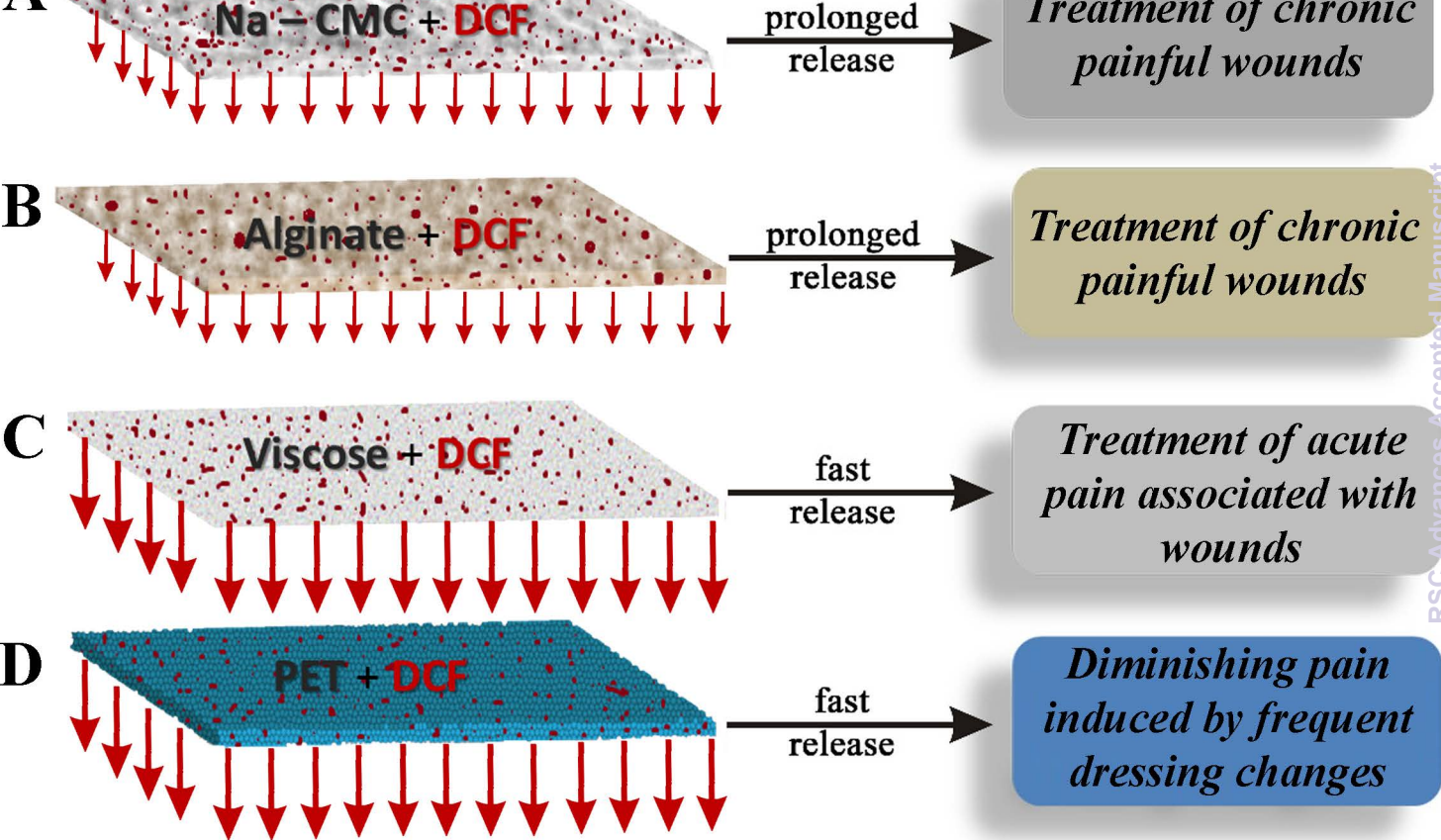


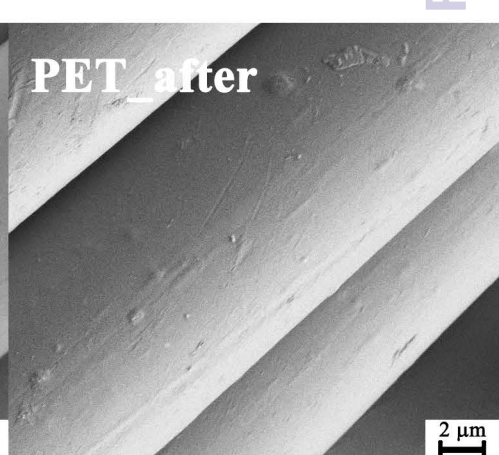
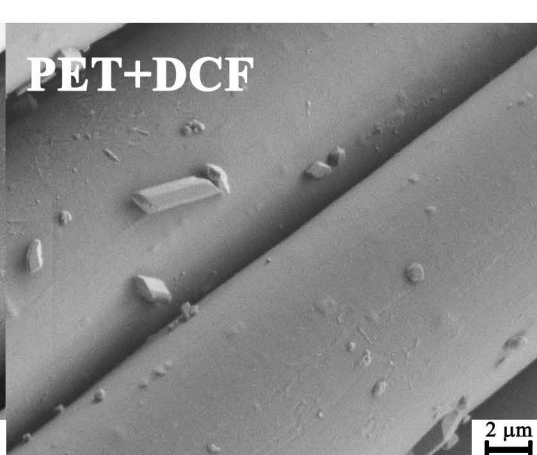
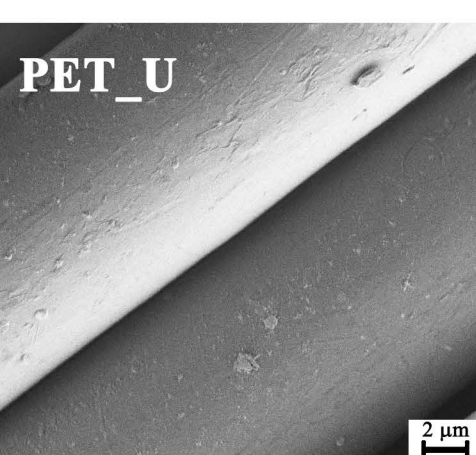
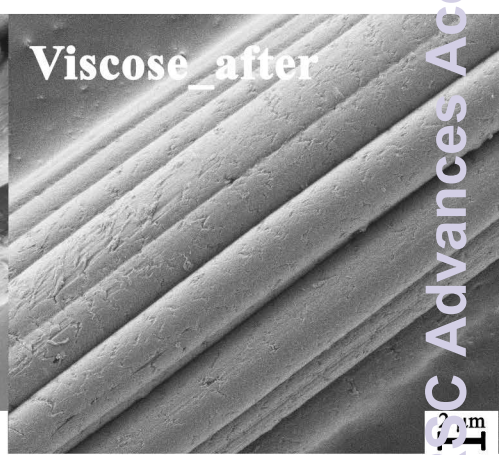
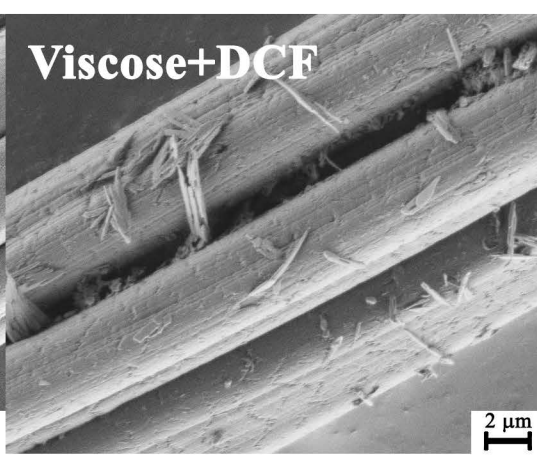
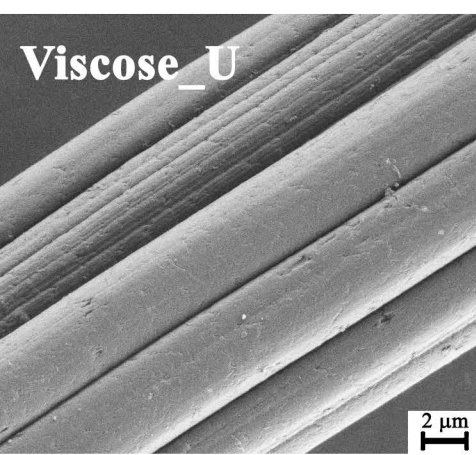
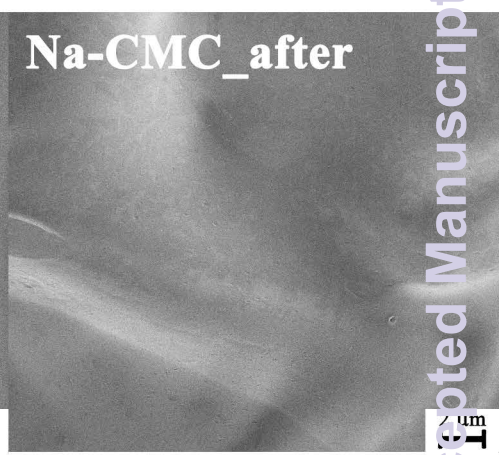
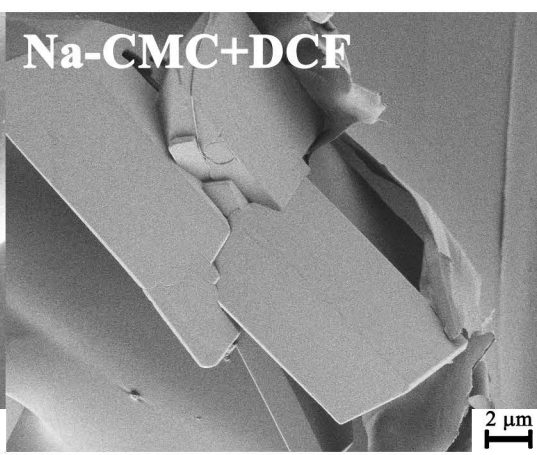
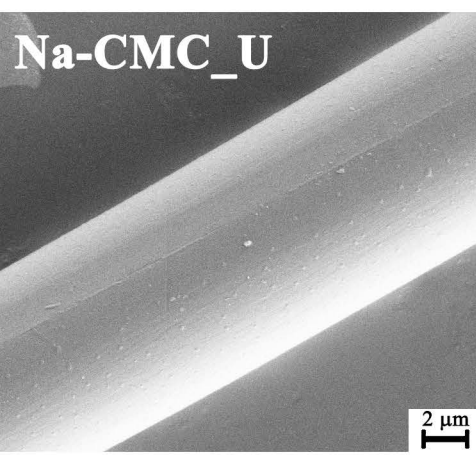
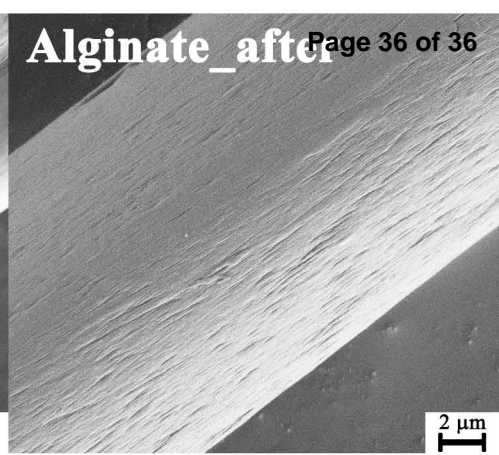
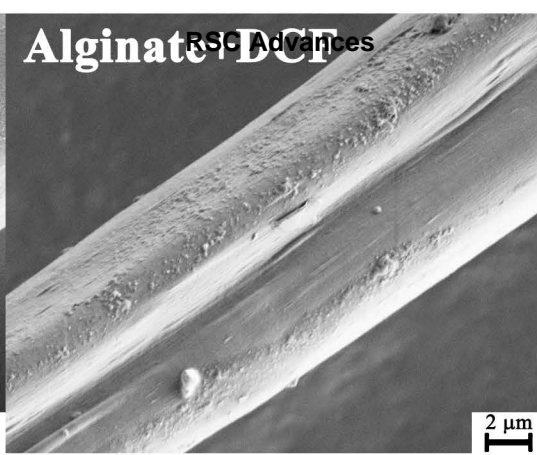
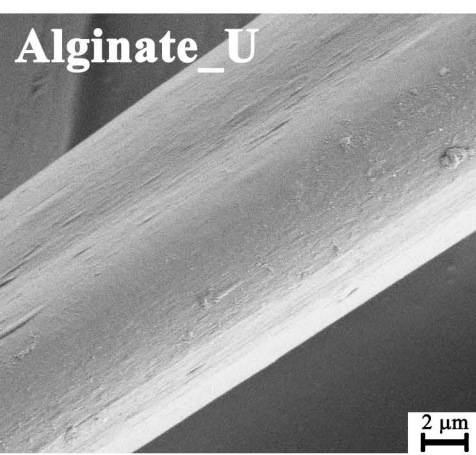




A**B**







RSC Advances Accepted Manuscript